

Tuning hole-injection barriers at organic/metal interfaces exploiting the orientation of a molecular acceptor interlayer

J. Niederhausen,¹ P. Amsalem,¹ J. Frisch,¹ A. Wilke,¹ A. Vollmer,² R. Rieger,³ K. Müllen,³ J. P. Rabe,¹ and N. Koch^{1,2,*}

¹Humboldt-Universität zu Berlin, Institut für Physik, Newtonstr. 15, DE-12489 Berlin, Germany

²Helmholtz Zentrum Berlin für Materialien und Energie GmbH - BESSY II, Albert-Einstein-Str. 15., DE-12489 Berlin, Germany

³Max Planck Institut für Polymerforschung, Ackermannweg 10, DE-55128 Mainz, Germany

(Received 24 April 2011; revised manuscript received 1 August 2011; published 3 October 2011)

Ultraviolet photoelectron spectroscopy was used to demonstrate organic/metal-contact charge injection barrier tuning by exploiting the orientation-dependent work function ϕ of a molecular acceptor [hexaazatriphenylene-hexanitrile (HATCN)] interlayer on Ag(111). The work function ϕ of a flat-lying HATCN monolayer on Ag was 4.6 eV (similar to a pristine Ag electrode), whereas a layer of edge-on HATCN on Ag exhibited ϕ of 5.5 eV (comparable to a pristine Au electrode). The hole-injection barriers (HIBs) between HATCN-modified electrodes and the organic semiconductors tris(8-hydroxyquinoline)aluminum (Alq₃) and N,N'-bis(1-naphthyl)-N,N'-diphenyl-1,1'-biphenyl-4,4'-diamine (α -NPD) were reduced by more than 1 eV compared to pristine Ag and Au electrodes. Noteworthy, the HIBs determined with the flat-lying HATCN interlayer were lower than those obtained for pristine Ag substrates (ϕ of both electrodes is 4.6 eV), and the HIBs with the edge-on HATCN on Ag were lower than those found for pristine Au (ϕ of both electrodes ca. 5.4 eV). This shows that acceptor interlayers are beneficial for charge injection in electronic devices even when the molecularly modified electrode ϕ is comparable to that of a pristine metal surface. It is argued that the molecularly modified electrodes are electronically more rigid than their pristine metal counterparts, i.e., the electron spill-out at the organic-terminated surface is less pronounced compared to Ag and Au surfaces.

DOI: [10.1103/PhysRevB.84.165302](https://doi.org/10.1103/PhysRevB.84.165302)

PACS number(s): 73.20.-r, 33.60.+q, 73.30.+y

I. INTRODUCTION

Interfaces between metals and conjugated organic materials have been the subject of fundamental and applied research for many years¹⁻³ because they are of importance for good charge injection in organic electronic devices. To achieve low contact resistance it is necessary to minimize the charge injection barriers that exist at interfaces formed by metal electrodes and organic semiconductors. A promising route toward optimizing electron (hole) injection barriers comprises the use of interlayers of strong molecular donors (acceptors).^{4,5} The donors (acceptors) can undergo a charge transfer reaction with the metal electrode, which modifies the metal surface charge distribution and this decreases (increases) the work function (ϕ). For instance, it was shown that ϕ of Cu, Ag, and Au can be adjusted continuously between 3.3 and 5.4 eV by proper choice of donor/acceptor molecule and the interlayer coverage (from submonolayer to full monolayer).⁴⁻⁷ Organic molecules and polymers deposited onto such modified metal electrodes realign their molecular levels with respect to the actual ϕ value, which allows minimizing the charge injection barriers for virtually any organic semiconductor. However, the structural variability of molecules in such interlayers demands further attention. Recently, it was shown that the electron acceptor hexaazatriphenylene-hexanitrile (HATCN), which can be employed as interlayer to increase ϕ of Ag and Cu, undergoes a density-dependent orientation transition in the monolayer regime.⁸ On Ag, for instance, HATCN first forms a flat lying monolayer, where the metal-to-molecule electron transfer^{1,2,8} balances the metal-surface electron “push-back” effect.^{1,9} Consequently, ϕ of flat-lying monolayer HATCN/Ag is the same as that of the pristine Ag surface (ca. 4.6 eV). Deposition of further HATCN molecules induces a transition to a denser monolayer of

almost upright-standing edge-on oriented HATCN molecules. This is accompanied by a different metal-to-molecule electron transfer and electron density distribution, which results in a high ϕ of a complete edge-on HATCN monolayer on Ag of 5.5 eV.⁸ Consequently, structural changes of such interlayers may have a significant impact on the actually achievable charge-injection barriers at metal/organic semiconductor contacts.

In this work, we use ultraviolet photoelectron spectroscopy (UPS) to examine the effect of HATCN molecular orientation in interlayers on Ag(111) on the resulting charge injection barriers toward N,N'-bis(1-naphthyl)-N,N'-diphenyl-1,1'-biphenyl-4,4'-diamine (α -NPD) and tris(8-hydroxyquinoline)aluminum (Alq₃), which are prototypical hole- and electron-transport materials in organic light emitting diodes. We find that the orientation of HATCN molecules in the interlayer significantly impacts the actual charge-injection barriers for both α -NPD and Alq₃. Moreover, we contrast the results from interlayer-modified metal electrodes with pristine metal electrodes of the same work function, i.e., Ag versus flat-lying HATCN/Ag and Au versus edge-on HATCN/Ag. This allows us to discuss the difference of surface electron spill-out for clean metal and interlayer-modified metal electrodes and its effect on the energy level alignment with organic semiconductors.

II. EXPERIMENTAL

All experiments were carried out at the multichamber ultrahigh vacuum (UHV) endstation SurICat (at beamline PM4) at BESSY II (Berlin, Germany). Clean Ag(111) surfaces were prepared by repeated Ar-ion sputtering and annealing cycles. α -NPD and Alq₃ were purchased from Sigma-Aldrich

Co. and used as received. HATCN was synthesized and purified at the MPI in Mainz. The molecular materials were sublimed from resistively heated pinhole sources. Substrates were held at room temperature and deposition rates were ca. 1 Å/min. The film thickness values given in the text are nominal mass-thickness values determined with a quartz crystal microbalance, not corrected for possible differences in sticking coefficient on the microbalance and the actual substrates. During evaporation the pressure never exceeded 5×10^{-8} mbar. Samples were transferred to the analysis chamber ($p = 5 \times 10^{-10}$ mbar) without breaking vacuum. UPS spectra were collected using a hemispherical electron energy analyzer (Scienta SES 100) and an excitation energy of 35 eV. The secondary electron cutoff (SECO) was measured with a sample bias voltage of -10 V to clear the analyzer work function. The energy position of SECOs and the low binding energy onset of emission from the highest occupied molecular level (to determine hole injection barriers) were determined by linear extrapolation of the respective peak at half maximum towards the background.

III. RESULTS AND DISCUSSION

A. α -NPD on pristine Ag and Au

The top part of Fig. 1(a) shows the valence spectra and the secondary electron cutoffs (SECO) for α -NPD deposited with incremental coverage on Ag(111). The values for the hole injection barrier (HIB) and ϕ determined from these spectra are summarized in Fig. 2—as are the ones for the other systems discussed in this text. ϕ of pristine Ag(111) was 4.60 eV. In the coverage range from 2 to 10 Å (spectra not shown), ϕ decreased linearly with coverage to 3.65 eV and remained constant for yet higher coverages, indicating the completion of the molecular monolayer at ca. 10 Å. The lowering of ϕ is due to a modification of the Ag surface dipole by the “push-back” effect, which corresponds to a compression of the electron tail spilling out of the clean metal surface.^{1,9}

The valence spectra show a distinct photoemission feature spanning from 1.4 to 2.7 eV binding energy (BE) for low α -NPD coverages. It consists of emission from the highest

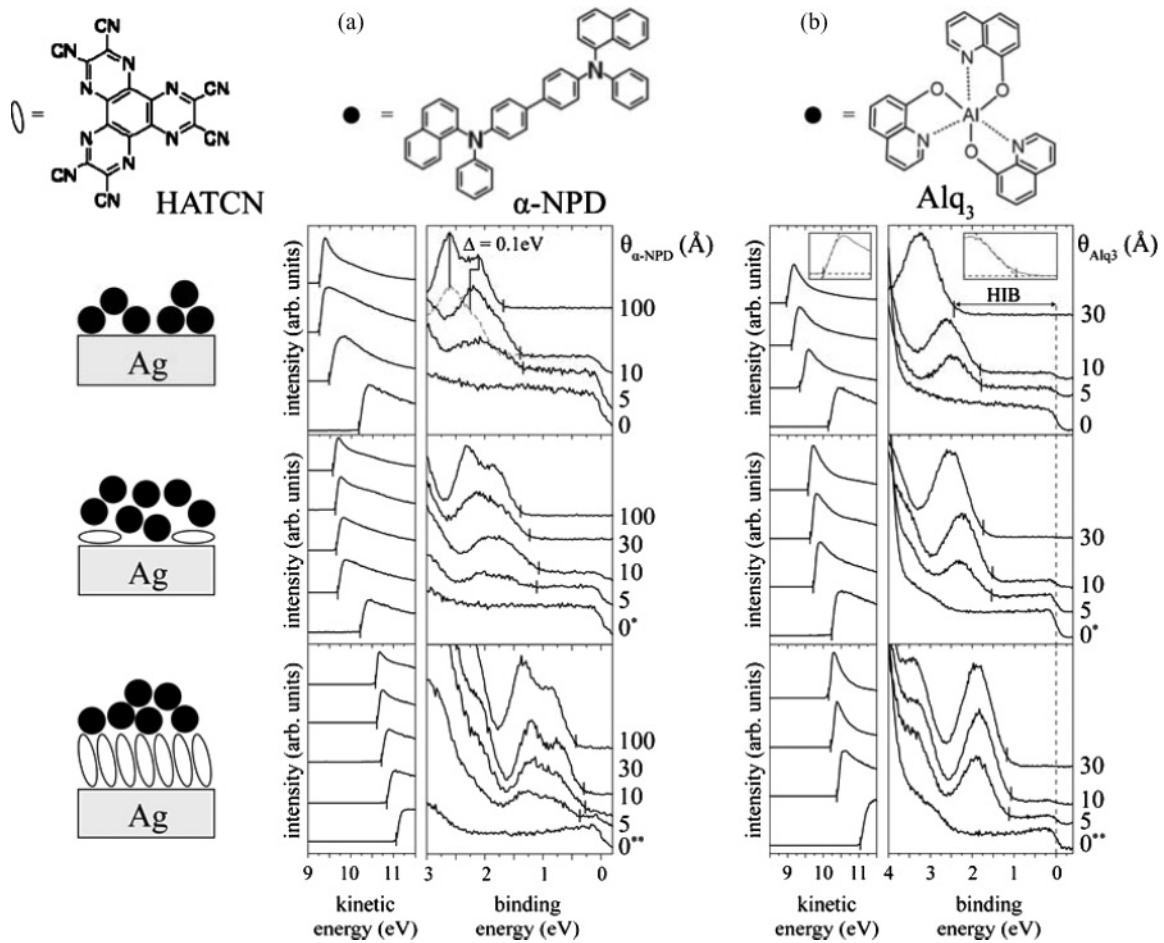


FIG. 1. UPS valence and SECO spectra for (a) α -NPD and (b) Alq_3 (thickness $\theta_{\alpha\text{-NPD}}$ and θ_{Alq_3} respectively) deposited on (from top to bottom) pristine Ag(111), flat-lying HATCN interlayer on Ag(111), and edge-on HATCN interlayer on Ag(111). The flat-lying and edge-on HATCN interlayer spectra are labeled 0^* and 0^{**} , respectively. The spectrum of 10 Å α -NPD/Ag(111) is also shown shifted (dashed gray) to illustrate the HOMO shift from mono- to multilayer. The insets for (b) show how the energy position of the SECO and the low binding energy onset of emission from the HOMO were determined at the example of 30 Å Alq_3 /Ag(111). The chemical structures of HATCN, α -NPD, and Alq_3 are shown in the upper row.

and second highest occupied molecular orbital (HOMO and HOMO-1).¹⁰ The HOMO low-energy onset is at 1.40 eV BE in the monolayer (ML) regime and undergoes a shift of 0.35 eV to higher BE for multilayers (see, e.g., 100 Å spectrum), i.e., the hole-injection barrier (HIB) from Ag into multilayer α -NPD is 1.75 eV. The constant ϕ when going from 10 to 100 Å coverage, indicates the absence of charging. Consequently, the observed shift predominantly results from a difference in the metal-substrate mediated photo-hole screening for α -NPD monolayer versus multilayer.^{1,2,11} However, the energy splitting between HOMO peak maximum and all other valence band features is apparently 0.1 eV larger in the α -NPD multilayer compared to the monolayer [indicated for the HOMO-1 by the thin lines in Fig. 1(a)].

As no interface states close to the Fermi-level (E_F) are observed, we conclude that the interaction between α -NPD and Ag(111) is rather weak, i.e., physisorptive rather than involving significant charge transfer or covalent bond formation. Consequently, the difference in the HOMO-HOMO-1 energy splitting does not reflect a chemical interaction, but is most likely due to different molecular properties in the monolayer versus multilayer. Similar observations were reported for *p*-sexiphenyl adsorbed on Ag(111)¹² and explained by a change in the twist angle of the phenyl units.¹³ In the case of α -NPD, the HOMO is localized on the central biphenyl core.¹⁰ Accordingly, our observed differential shift would correlate to an increased twist of the biphenyl unit in the monolayer because the HOMO is at higher BE. This suggests that the interaction of α -NPD with the Ag surface is predominately mediated by the phenyl or naphthyl end-groups,

which would be enabled by an increased biphenyl inter-ring twist angle. However, another mechanism may cause apparent changes of peak maxima in photoemission from molecular materials.¹⁴ The strength of electron-vibron coupling, which governs the intensity distribution of vibronic replica on the high BE side of the vibronic ground-state transition, may be different for mono- and multilayer. Consequently, the apparent shift in the maximum of emission from the α -NPD HOMO may be due to a larger Huang-Rhys factor¹⁵ for the monolayer that interacts directly with the metal substrate. The HIB and ϕ values determined from the spectra are summarized in the schematic energy level diagrams of Fig. 2.

The electronic structure of α -NPD on Au investigated by UPS was reported in detail by Wan *et al.*,¹⁶ and we shortly review their most important findings in the following. For multilayers, the HIB was 1.4 eV and ϕ of the molecule-covered Au was 4.1 eV, i.e., 1.3 eV lower than ϕ of the pristine Au. The differences found for the ϕ -change and HIB for α -NPD on the two metals mainly reflects the difference in the specifics of the “push-back” of Ag versus Au. Noteworthy, while ϕ values of the pristine metal surfaces differ by 0.8 eV, HIB values (for multilayers) differ only by 0.35 eV. We now turn toward α -NPD deposited on HATCN precovered Ag(111). Two different precoverages were chosen: (i) 2 Å HATCN corresponding to a flat-lying monolayer with a ϕ value of 4.65 eV [essentially the same as pristine Ag(111)], and (ii) 12 Å HATCN corresponding to an edge-on monolayer with a ϕ value of 5.50 eV [essentially the same as pristine Au(111)].

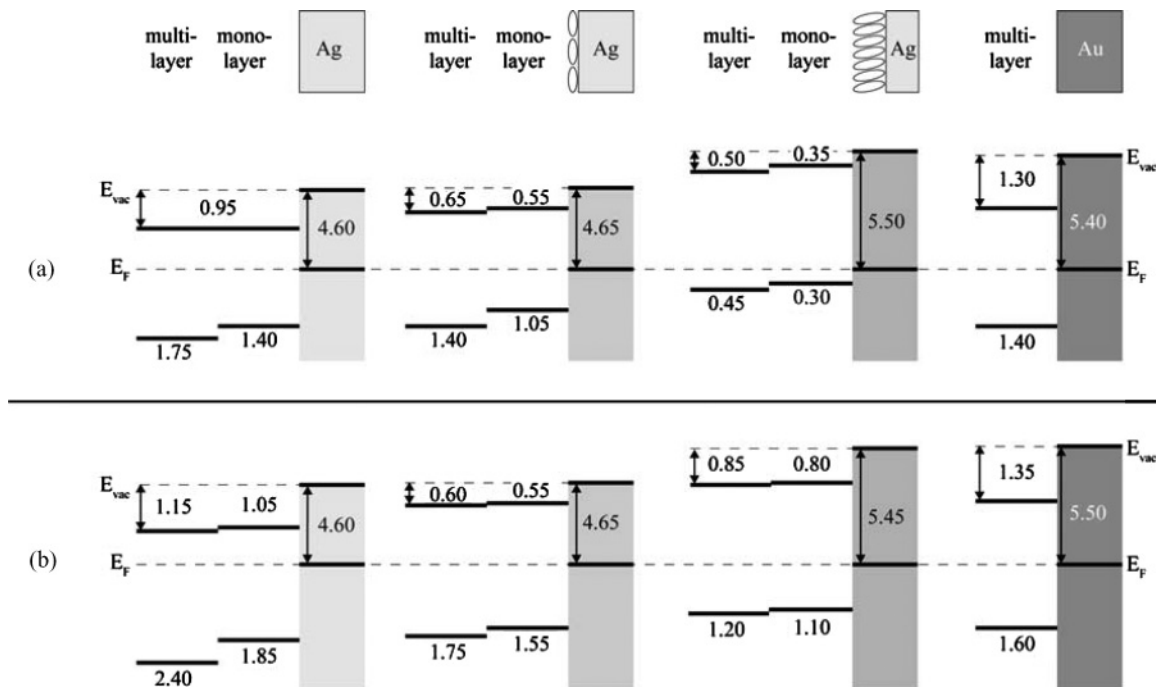


FIG. 2. Schematic energy level diagrams of (a) α -NPD and (b) Alq_3 on (columns from left to right) pristine Ag(111), flat-lying HATCN interlayer on Ag(111), edge-on HATCN interlayer on Ag(111), and Au [polycrystalline Au for α -NPD (data taken from Ref. 16) and Au(111) for Alq_3 (data taken from Ref. 5)]. Note that to minimize effects of the permanent molecular dipole moment of Alq_3 , a nominal coverage of 30 Å was chosen as multilayer for the respective systems. This is in contrast to the α -NPD results for which the multilayers have a nominal coverage of 100 Å.

B. α -NPD on the flat-lying HATCN interlayer

The coverage-dependent valence and SECO spectra for α -NPD deposited on Ag(111) with a flat-lying HATCN interlayer are displayed in the middle part of Fig. 1(a). The valence region of this layer exhibits a weak and broad feature spreading from ~ 1.3 eV BE up to E_F . These states have been assigned to LUMO-derived hybrid states also involving a contribution from the Ag bands, which is partially filled due to metal-to-molecule electron charge transfer. Upon adsorption of 2 Å HATCN, ϕ remains unchanged because the “push-back” effect is counterbalanced by the charge transfer.¹⁷ The structure of the flat-lying interlayer is characterized by flat-lying HATCN molecules in a honeycomb arrangement where uncovered Ag patches are exposed via nanocavities.¹⁷

For from circa a half up to a full monolayer (5 and 10 Å, respectively) of α -NPD deposited on the flat-lying HATCN interlayer, ϕ decreased by 0.55 eV and the HOMO low-BE onset was at 1.05 eV. The overall ϕ reduction upon multilayer α -NPD deposition was 0.65 eV, and the HOMO onset shifted to 1.40 eV BE. The observed ϕ decrease upon α -NPD deposition is 0.3 eV smaller than for pristine Ag(111), but not zero as might be expected for noninteracting molecule-molecule interfaces. This behavior may be explained by considering that α -NPD partially adsorbs on the free Ag patches (the nanocavities of the HATCN honeycomb structure), which leads to a “push-back”, however, reduced in magnitude as most of the surface is covered by HATCN. Upon adsorption of multilayer α -NPD, the HOMO onset shifted toward higher BE by 0.35 eV, as expected for decreased photo-hole screening. Compared to α -NPD/Ag(111), where the VB shifted by 0.45 eV to higher BE, we now find a reduction of the substrate-induced screening by 0.10 eV. This might be due to the lower screening efficiency of the HATCN interlayer compared to the metal.

C. α -NPD on the edge-on HATCN interlayer

The second interlayer that we investigated comprised nominal 12 Å HATCN coverage on Ag(111), which equals to an edge-on HATCN monolayer. Due to the different bonding pattern, this interlayer increases ϕ to 5.50 eV compared to 4.60 eV for pristine Ag(111).⁸ This will enable a good comparison to the results obtained on pristine Au with a very similar ϕ (5.40 eV, see above). Coverage-dependent photoemission spectra of α -NPD grown on edge-on HATCN/Ag(111) are displayed in the bottom part of Fig. 1(a). The total ϕ decrease, up to 100 Å α -NPD coverage, was only 0.50 eV. The HOMO-onset was at 0.3 eV for the α -NPD monolayer and it shifted to 0.45 eV BE for the multilayer.

The ϕ and HIB values that we found for α -NPD on edge-on HATCN/Ag(111) directly indicate that the energy level alignment at this interface is governed by Fermi-level pinning.^{18–20} This substrate’s ϕ (5.50 eV) is larger than the ionization energy (IE) of α -NPD (5.20–5.45 eV). If vacuum level alignment occurred, the HOMO of α -NPD would be placed above E_F , i.e., a situation out of thermodynamic equilibrium. In the integer charge transfer model for pinning, electron transfer from α -NPD into the substrate occurs, which leads to an interface dipole that pulls the occupied levels of the organic overlayer below E_F to establish equilibrium.¹⁸ The

interfacial charge transfer is thus accompanied by energetically relaxed positive polaron formation in the α -NPD monolayer, which yields the low HIB of 0.3 eV; with increasing coverage, the HOMO-onset shifts to 0.45 eV, i.e., the BE for neutral molecules in the multilayer. Fully analogous observations were reported for the E_F -pinning behavior of diindenoperylene on high- ϕ conductive polymer electrodes.¹⁹ In addition, part of this shift may be due to the reduced screening by the underlying HATCN/Ag as the film thickness increases. Consistently, the final sample ϕ of 5.0 eV found here corresponds to the ϕ value that defines the border between E_F -pinning and the Schottky-Mott limit for α -NPD.^{18,20} Another mechanism that could explain pinning was recently put forward by Rissner *et al.*²¹ Here, no long-range charge transfer between the pinned molecular overlayer and substrate is involved, but rather a charge-density rearrangement within the α -NPD layer due to polarization may cause the interface dipole that brings the system to equilibrium. At present, experimental evidence for either integer charge transfer or polarization as the cause for pinning is not available and these two mechanisms are being discussed controversially.

D. Alq₃ on the HATCN interlayers and comparison to α -NPD

Alq₃, which has a similar IE as α -NPD (5.8 eV as compared to 5.4 eV), was used as another molecular overlayer in order to validate the generality of the observed effect of the HATCN interlayer. The corresponding spectra are shown in Fig. 1(b) and the characteristic energy level values are summarized in Fig. 2(b). The values for Alq₃/Au(111) are from literature.⁵ ϕ for multilayer Alq₃ was 3.45 eV (4.15 eV) in case of the bare Ag (Au) substrate. These values are similar to those found for α -NPD, which suggests a “push-back” effect of comparable magnitude for both molecules. Due to the higher IE of Alq₃, the HIB is generally larger than for α -NPD. On Ag, it is 1.85 eV for the ML and amounts to 2.40 eV for the multilayer. This yields a screening-induced difference of 0.55 eV, which may include a small contribution from the permanent intramolecular dipole of Alq₃. On Au, the HIB for a 30 Å Alq₃ film is 1.60 eV.

For Alq₃ deposited on silver precovered with flat-lying HATCN (initial ϕ of 4.65 eV), ϕ is 4.05 eV. This ϕ change of 0.6 eV is almost the same as for α -NPD. This is expected, as the adsorption in the remaining HATCN-uncovered Ag surface area should induce a similar “push-back” effect for the two molecules. The HIB of Alq₃ on flat-lying HATCN/Ag(111) is 1.55 eV for the monolayer, i.e., 0.30 eV lower compared to the bare Ag electrode. For the edge-on HATCN interlayer (initial ϕ of 5.45 eV), ϕ reduces upon adsorption of Alq₃ by 0.85 eV, giving a final ϕ of 4.6 eV. The HIB of Alq₃ is 1.10 eV for the ML and 1.20 eV for the multilayer. The significant ϕ decrease observed for Alq₃ deposited on edge-on HATCN/Ag(111) points towards E_F -pinning on this high- ϕ substrate. However, the HIB of 1.10–1.20 eV seems rather high compared to α -NPD. Nonetheless, HIB values of this magnitude in the pinning regime can yet be rationalized when deep intragap states in the organic semiconductor are present.²² In fact, for Alq₃, we find the pinning level to be 1.10 eV for the ML. A similar HIB value (1.2 eV) was found for a ML of Alq₃ on the conductive polymer poly(ethylenedioxythiophene):poly(styrenesulfonate)

(PEDOT:PSS with a $\phi = 5.1$ eV) and attributed to pinning at gap states with a density too low to be directly observed in UPS.²³

In essence, the qualitative behavior of Alq₃ on Ag, Au, and the two flat-lying and edge-on HATCN interlayers on Ag parallels that of α -NPD, providing solid support for the general validity of the concepts for the application of interlayers that we discuss in the following.

The flat-lying HATCN interlayer features essentially the same ϕ value as pristine Ag(111) (ca. 4.6 eV), and ϕ of the upright-standing HATCN layer resembles that of Au (ca. 5.5 eV). However, the HIB values determined for α -NPD and Alq₃ on electrodes with comparable ϕ with and without the acceptor interlayer differ notably. In both cases, the HIB is significantly lower when HATCN interlayers are present, which is also reflected by smaller ϕ -changes resulting from deposition of the organic semiconductor (see Fig. 2). For instance, ϕ decreases by 1.3 eV for α -NPD on Au, whereas the decrease is only 0.5 eV when an edge-on HATCN interlayer on Ag(111) is used as electrode. Note that part of this 0.5 eV ϕ decrease is due to E_F pinning, and might be even smaller if pinning did not occur. As noted above, the ϕ decrease for weakly adsorbed organic molecules on clean metal surfaces is due to the “push-back” effect, i.e., the electron density spilling out into vacuum at the free metal surface is partially moved back into the metal due to Pauli repulsion.²⁴ A similar effect may be operative for the HATCN-covered Ag surfaces as well; however, greatly reduced in magnitude as the α -NPD- and Alq₃-induced ϕ decrease is much smaller. Consequently, it appears that the mechanically “soft matter” molecular

interlayer is electronically more rigid than the “hard matter” Ag and Au.

IV. CONCLUSION

In conclusion, HATCN interlayers of two different orientations on Ag(111) were employed to tune the energy level alignment at organic semiconductor/metal electrode interfaces. Ultraviolet photoelectron spectroscopy experiments revealed that employing such acceptor interlayers significantly reduced the hole-injection barriers for organic semiconductors, up to 1.3 eV for α -NPD and up to 1.2 eV for Alq₃, compared to pristine Ag. Most notably, even when the acceptor-modified electrodes exhibited the same ϕ as pristine metal surface [flat-lying HATCN/Ag(111) and Ag(111), and edge-on HATCN/Ag(111) and Au] substantial HIB reductions were accomplished through the mere presence of the acceptor interlayer. This is attributed to a more rigid character of the surface electron density of the metal-adsorbed HATCN layers compared to the electronically “soft” surface of metals, where considerable electron density spills out into vacuum. Consequently, the electron “push-back” effect due to the deposition of an organic semiconductor is less pronounced for molecularly modified metal electrodes, which is beneficial for their use as charge-injection contacts in organic electronic devices.

ACKNOWLEDGMENTS

We gratefully acknowledge financial support by the DFG.

*norbert.koch@physik.hu-berlin.de

- ¹I. Ishii, K. Sugiyama, E. Ito, and K. Seki, *Adv. Mater.* **11**, 605 (1999).
²A. Kahn, N. Koch, and W. Gao, *J. Polym. Sci. Polym. Phys.* **41**, 2529 (2003).
³N. Koch, *J. Phys. Condens. Matter* **20**, 184008 (2008).
⁴N. Koch, S. Duhm, J. P. Rabe, A. Vollmer, and R. L. Johnson, *Phys. Rev. Lett.* **95**, 237601 (2005).
⁵B. Bröker, R.-P. Blum, J. Frisch, A. Vollmer, O. T. Hofmann, R. Rieger, K. Müllen, J. P. Rabe, E. Zojer, and N. Koch, *Appl. Phys. Lett.* **93**, 243303 (2008).
⁶L. Romaner, G. Heimel, J.-L. Brédas, A. Gerlach, F. Schreiber, R. L. Johnson, J. Zegenhagen, S. Duhm, N. Koch, and E. Zojer, *Phys. Rev. Lett.* **99**, 256801 (2007).
⁷G. M. Rangger, O. T. Hofmann, B. Bröker, and E. Zojer, *Synth. Meter.* **160**, 1456 (2010).
⁸B. Bröker, O. T. Hofmann, G. M. Rangger, P. Frank, R.-P. Blum, R. Rieger, L. Venema, A. Vollmer, K. Müllen, J. P. Rabe, A. Winkler, P. Rudolf, E. Zojer, and N. Koch, *Phys. Rev. Lett.* **104**, 246805 (2010).
⁹G. Witte, S. Lukas, P. S. Bagus, and C. Wöll, *Appl. Phys. Lett.* **87**, 263502 (2005).
¹⁰I. G. Hill, A. Kahn, J. Cornil, D. A. dos Santos, and J.-L. Brédas, *Chem. Phys. Lett.* **317**, 444 (2000).
¹¹I. G. Hill, A. J. Mäkinen, and Z. H. Kafafi, *J. Appl. Phys.* **88**, 889 (2000).
¹²N. Koch, G. Heimel, J. Wu, E. Zojer, R. L. Johnson, J.-L. Brédas,

- K. Müllen, and J. P. Rabe, *Chem. Phys. Lett.* **413**, 390 (2005).
¹³J.-L. Brédas, G. B. Street, B. Thémans, and J. M. André, *J. Chem. Phys.* **83**, 1323 (1985).
¹⁴H. Yamane, S. Nagamatsu, H. Fukagawa, S. Kera, R. Friedlein, K. K. Okudaira, and N. Ueno, *Phys. Rev. B* **72**, 153412 (2005).
¹⁵N. E. Gruhn, D. A. da Silva Filho, T. G. Bill, M. Malagoli, V. Coropceanu, A. Kahn, and J.-L. Brédas, *J. Am. Chem. Soc.* **124**, 7918 (2002).
¹⁶A. Wan, J. Hwang, F. Amy, and A. Kahn, *Org. Electron.* **6**, 47 (2005).
¹⁷H. Glowatzki, B. Bröker, R.-P. Blum, O. T. Hofmann, A. Vollmer, R. Rieger, K. Müllen, E. Zojer, J. P. Rabe, and N. Koch, *Nano Lett.* **8**, 3825 (2008).
¹⁸S. Braun, W. Osikowicz, Y. Wang, and W. R. Salaneck, *Org. Electron.* **8**, 14 (2007).
¹⁹J. Wagner, M. Gruber, A. Hinderhofer, A. Wilke, B. Bröker, J. Frisch, P. Amsalem, A. Vollmer, A. Opitz, N. Koch, F. Schreiber, and W. Brütting, *Adv. Funct. Mater.* **20**, 4295 (2010).
²⁰N. Koch and A. Vollmer, *Appl. Phys. Lett.* **89**, 162107 (2006).
²¹F. Rissner, G. M. Rangger, O. T. Hofmann, A. M. Track, G. Heimel, and E. Zojer, *ACS Nano* **3**, 3513 (2009).
²²T. Sueyoshi, H. Fukagawa, M. Ono, S. Kera, and N. Ueno, *Appl. Phys. Lett.* **95**, 183303 (2009).
²³A. S. Wan, A. J. Mäkinen, P. A. Lane, and G. P. Kushto, *Chem. Phys. Lett.* **446**, 317 (2007).
²⁴P. S. Bagus, K. Hermann, and C. Wöll, *J. Chem. Phys.* **123**, 184109 (2005).